Title

ORIGINAL ARTICLE: Facilitating glaucoma diagnosis with inter-eye neuroretinal rim asymmetry analysis using spectral domain optical coherence tomography

Journal

Digital Journal of Ophthalmology, 28(4)

ISSN

1542-8958

Authors

Taliaferro, Andrew S
Fayed, Mahmoud A
Tsikata, Edem
et al.

Publication Date

2022

DOI

10.5693/djo.01.2022.10.001

Peer reviewed

DJO Digital Journal of Ophthalmology
www.djo.harvard.edu

Original Article

Facilitating glaucoma diagnosis with intereye neuroretinal rim asymmetry analysis using spectral-domain optical coherence tomography

Andrew S. Taliaferro, MD,[a,b] **Mahmoud A. Fayed, MD**,[a,b] **Edem Tsikata, PhD**,[a,b] **Regina A. De Luna, MD**,[a,b] **Firas Jassim, PhD**,[a,b] **Sumir Pandit, MD, MBA**,[a,b] **Elli A. Park, MD**,[a,b] **Maria A. Guzman Aparicio, MD**,[a,b] **Linda Yi-Chieh Poon, MD**,[a,b] **Christian Que, MD**,[a,b] **Huseyin Simavli, MD**,[a,b] **Vivek Srinivasan, PhD**,[c] **Johannes F. de Boer, PhD**,[d,e] and **Teresa C. Chen, MD**[a,b]

Author affiliations: [a]*Harvard Medical School, Boston, Massachusetts;*

[b]*Department of Ophthalmology, Glaucoma Service, Massachusetts Eye and Ear, Boston, Massachusetts;*

[c]*Martinos Center for Biomedical Imaging, Massachusetts General Hospital, Boston, Massachusetts;*

[d]*LaserLaB Amsterdam, Department of Physics and Astronomy, Vrije Universiteit, Amsterdam, The Netherlands;*

[e]*Department of Ophthalmology, Amsterdam University Medical Centers, Amsterdam, The Netherlands*

Abstract

Purpose—To determine whether intereye asymmetry of a three-dimensional neuroretinal rim parameter, the minimum distance band, is useful in differentiating normal eyes from those with open-angle glaucoma.

Materials and Methods—This is a cross-sectional study of 28 normal subjects and 33 glaucoma subjects. Subjects underwent spectral domain optical coherence tomography imaging of both eyes. From high-density raster scans of the optic nerve head, a custom-designed segmentation algorithm calculated mean minimum distance band neuroretinal rim thickness globally, for four quadrants, and for four sectors. Intereye minimum distance band thickness asymmetry was calculated as the absolute difference in minimum distance band thickness values between the right and left eyes.

Results—Increasing global minimum distance band thickness asymmetry was not associated with increasing age or increasing refractive error asymmetry. Glaucoma patients had thinner mean neuroretinal rim thickness values compared to normal patients (209.0 μm vs 306.0 μm [$P < 0.001$]). Glaucoma subjects had greater intereye thickness asymmetry compared to normal subjects for the global region (51.9 μm vs 17.6 μm [$P < 0.001$]) as well as for all quadrants and all sectors. For detecting glaucoma, a thickness asymmetry value >28.3 μm in the inferior quadrant yielded the greatest sum of sensitivity (87.9%) and specificity (75.0%). Globally, thickness asymmetry >30.7 μm yielded the greatest sum of sensitivity (66.7%) and specificity (89.3%).

Conclusions—This study indicates that intereye neuroretinal rim minimum distance band asymmetry measurements, using high-density spectral domain optical coherence tomography volume scans, may be an objective and quantitative tool for assessing patients suspected of open-angle glaucoma.

Published December 26, 2022.

doi:10.5693/djo.01.2022.10.001

Correspondence: Teresa C. Chen, MD, Department of Ophthalmology, Glaucoma Service, Massachusetts Eye and Ear Infirmary, 243 Charles Street, Boston, MA 02114 (email: teresa_chen@meei.harvard.edu).

Financial support: Teresa C. Chen has received funding from the American Glaucoma Society Mid-Career Award, Massachusetts Lions Eye Fund, National Institutes of Health Award UL 1RR 025758, and Fidelity Charitable Fund (Harvard University). The sponsors or funding organizations had no role in the design or conduct of this research.

Disclosures: J.F. de Boer: Licenses to and royalty income from NIDEK Inc, Terumo Corporation, and Heidelberg Engineering. V. Srinivasan received royalties from Optovue Inc, Freemont, CA.

Digital Journal of Ophthalmology, Vol. 28

Digital Journal of Ophthalmology, Vol. 28

Glaucoma is the leading cause of irreversible blindness worldwide, and early diagnosis and treatment can prevent irreversible vision loss. Intereye cup-disc ratio asymmetry is an early hallmark of open-angle glaucoma (OAG). Spectral domain optical coherence tomography (SDOCT) can objectively quantify optic nerve measurements.[1] Although studies that have included glaucoma patients have found intereye asymmetry of retinal nerve fiber layer (RNFL) thickness, macular thickness, and retinal vessel density to be sensitive and specific markers of OAG,[2–8] only a single study has evaluated normal intereye asymmetry of the neuroretinal rim in healthy adults.[9] This study concluded that intereye differences in global Bruch's membrane opening-minimum rim width (BMO-MRW) do not exceed 49 μm in a population of healthy Brazilian subjects.[9] To our knowledge, the current study is the first SD-OCT study to evaluate intereye rim asymmetry in both normal and OAG patients in a multiethnic population. Specifically, this study uses the minimum distance band (MDB) neuroretinal rim measurement to assess for rim asymmetry.

The MDB is a high-density SD-OCT version of the commercially available low-density BMO-MRW; it quantifies neuroretinal rim tissue in three-dimensional (3D) space by measuring the shortest distance between the retinal pigment epithelium-Bruch's membrane (RPE-BM) complex and the internal limiting membrane (ILM), or cup surface. This 3D band represents the smallest cross-sectional area through which all ganglion nerve axons must pass to enter the optic nerve.[10,11] Besides having good structure function correlation and good diagnostic ability,[10–13] the MDB neuroretinal rim measurement not only outperforms current clinical structural testing (ie, disc photographs and RNFL thickness) by 1–2 years[14] but also results in fewer unusable or inaccurate glaucoma OCT test results (ie, only 15.8% vs 61.7% with commercially available software).[15,16] Furthermore, Kim et al[17] demonstrated that the MDB neuroretinal rim thickness was the most reproducible of five neuroretinal rim parameters studied (3D MDB thickness, 3D MDB area, 3D rim volume, 2D rim area, and 2D rim thickness). There are two key differences between the MDB and the BMO-MRW. First, the MDB parameter uses a high-density optic nerve volume scan (193 B-scans arranged in a raster pattern), whereas the commercially available BMO-MRW uses a low-density optic nerve volume scan (24 B-scans arranged in a radial pattern). Second, the MDB disc border is defined as the RPE/BM, whereas the BMOMRW disc border is defined as the BMO. Because the RPE/BM composite is more easily seen on SD-OCT scans than BMO alone, the MDB disc border is easier to segment than the BMO-MRW disc border (Figure 1).[18] In this study, we used custom-designed software to measure MDB thickness globally, for four quadrants and four sectors, using high-density volume scans obtained with the Spectralis SD-OCT machine (Heidelberg Engineering, Heidelberg, Germany) to determine whether intereye MDB neuroretinal rim asymmetry is useful in differentiating subjects with normal eyes from subjects with OAG.

Materials and Methods

Inclusion and Exclusion Criteria

Participants were recruited retrospectively from the prospective SD-OCT in Glaucoma Study at the Massachusetts Eye and Ear Glaucoma Service between April 2009 and July 2014. The study was approved by the Massachusetts Eye and Ear Institutional Review Board and adhered to the tenets of the Declaration of Helsinki and the US Health Insurance Portability and Accountability Act of 1996. Written informed consent had been obtained from all subjects for the previous prospective study.

All subjects underwent ophthalmologic examination by a glaucoma specialist (TCC), including best-corrected visual acuity, slit lamp biomicroscopy, Goldmann applanation tonometry, gonioscopy, and dilated funduscopy, from which cup-disc ratios were estimated using a 90 diopter (D) lens. Testing included disc photography (Visucam ProNM, Carl Zeiss Meditec Inc, Dublin, CA), central corneal thickness measurements (PachPen pachymeter, Accutome Ultrasound Inc, Malvern, PA), visual fields performed using the Swedish Interactive Threshold Algorithm 24-2 test of the Humphrey Visual Field Analyzer 750i (Carl Zeiss Meditec Inc, Dublin, CA), and SD-OCT imaging, which took place on the same day.

Overall inclusion criteria for normal and OAG subjects were age between 40 and 90 years, spherical equivalent of ± 5 D or better in both eyes, and reliable visual fields (ie, ≤33% fixation losses, ≤20% false positives, and ≤20% false negatives).[4] Overall exclusion criteria were signal strength ≤15 on SD-OCT imaging, monocular status, factors that would preclude high-quality imaging (ie, media opacities or a dilated pupil of <2 mm), and history of cataract surgery within 3 months of imaging or other intraocular surgery within 6 months of imaging.

Normal patients did not have any eye disease other than mild cataract. Patients were excluded if cup-disc ratios were >0.4 for white patients and >0.6 for black or Hispanic patients. Race and ethnicity of patients were deter-

Digital Journal of Ophthalmology, Vol. 28

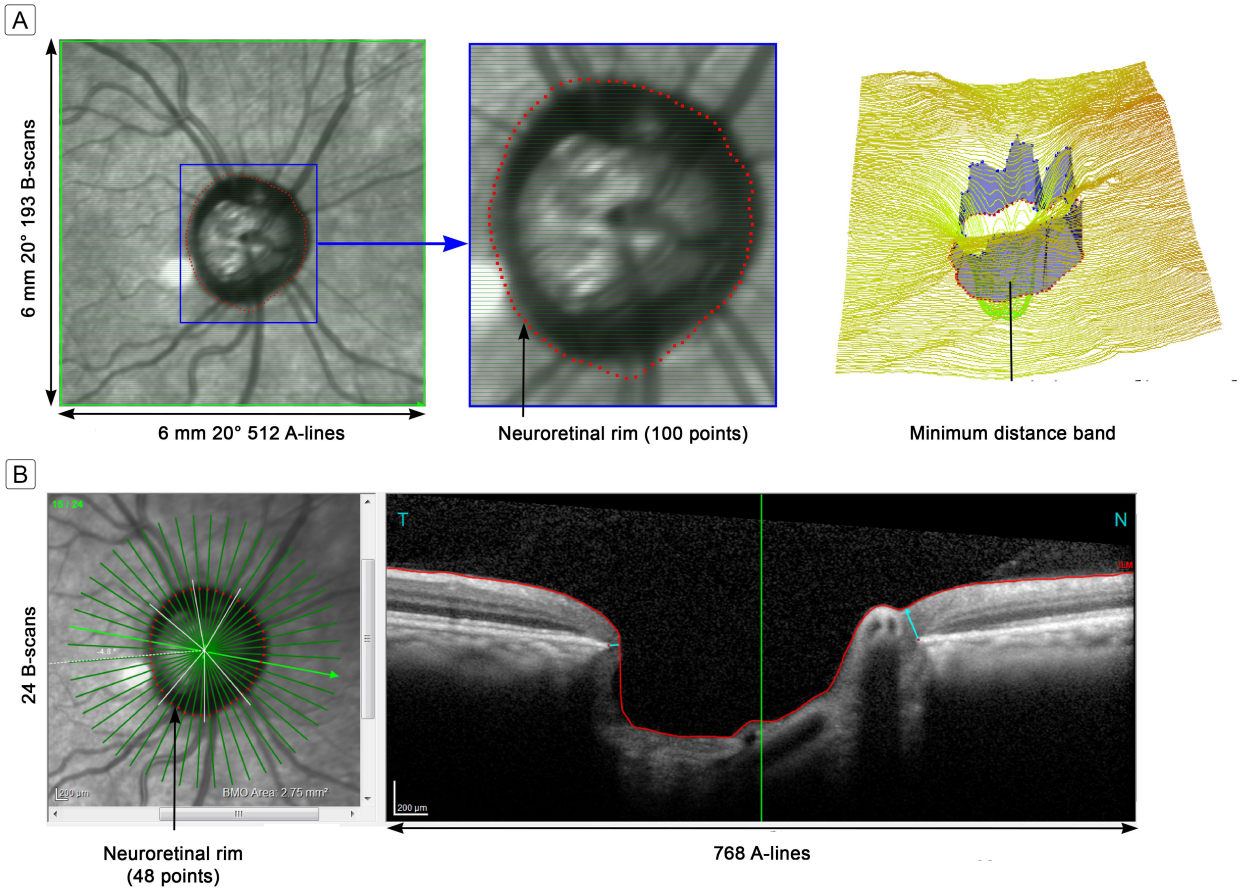

Figure 1. Two three-dimensional neuroretinal rim parameters in a normal patient: the minimum distance band (MDB) parameter and the Bruch's membrane opening–minimum rim width (BMO-MRW) parameter. A, Scan protocol for minimum distance band (MDB) thickness determinations is a 193 raster B-scan protocol, from which scan two concentric borders are reconstructed: (1) the OCT-based disc border, identified by the 100 points that correlate with the retinal pigment epithelium/Bruch's membrane (RPE/BM) complex (red dots, left and center), and (2) the internal limiting membrane or cup surface (blue dots, right). The MDB neuroretinal rim is the shaded area between these two concentric borders and represents the shortest distance between these two borders. B, Scan protocol for the Bruch's membrane opening–minimum rim width (BMO-MRW) parameter is a 24-line radial scan, from which two concentric borders are reconstructed: (1) the OCT-based disc border, identified by 48 points that correlate with Bruch's membrane opening (red dots), and (2) the cup surface (red line, right). The BMO-MRW is the circumferential band delimited by the shortest distance between these two borders.

mined during their visit with the glaucoma specialist. Additional inclusion criteria for normal subjects were best-corrected visual acuity 20/40 or better in both eyes, intereye cup-disc ratio asymmetry of <0.2, normal visual field test with pattern standard deviation >5%, and glaucoma hemifield test within normal limits. The intereye cup-disc ratio asymmetry <0.2 inclusion criteria was used to not inadvertently include any pre-perimetric glaucoma patients with mild intereye cup-disc ratio asymmetry into the normal group. Additional exclusion criteria for normal subjects were previous history of intraocular pressure >22 mm Hg in either eye.[4]

OAG subjects were included if they had a confirmed OAG diagnosis in both eyes, based on characteristic glaucomatous optic disc abnormalities with corresponding abnormal visual field defects. A visual field test was defined as abnormal if three or more contiguous test locations in the pattern standard deviation plot were depressed significantly at P <0.05 level, with at least one of these at the P <0.01 level on the same side of the horizontal meridian.[19] Glaucoma staging was modeled after the Hodapp-Anderson-Parrish criteria: early glaucoma (−6 dB ≤ mean deviation [MD] ≤ 0 dB), moderate glaucoma (−12 dB ≤ MD < −6 dB), and advanced glaucoma (MD < −12 dB). Any abnormal points in the outer perimeter of the Humphrey visual field plot were excluded to avoid potential rim artifacts.

Digital Journal of Ophthalmology, Vol. 28

3D Volume Imaging of the Optic Nerve

All subjects underwent Spectralis SD-OCT imaging by an experienced eye technician after pupillary dilation with phenylephrine 5% and tropicamide 0.5% drops. Each eye underwent the 12° circular peripapillary RNFL scan and the high-density 3D volume scan, comprising 193 B-scans centered on the optic nerve.

Image Segmentation of the Neuroretinal Rim

The MDB neuroretinal rim algorithm automatically segments the ILM and the RPE/BM complex in the 193 B-scans and then reconstructs the neuroretinal rim in 3D space by measuring the closest distance between the ILM and RPE/BM. The custom-designed software also allows for manual deletion of poorly segmented images and subsequent automated correction of segmentation errors. Intereye MDB thickness asymmetry was calculated globally and for each quadrant and sector, as the absolute difference in mean MDB thickness for a given region between the right and left eyes.

Statistical Analysis

Demographics and ocular characteristics of the normal and glaucoma groups were compared using χ^2 tests for categorical variables and *t* tests for continuous variables. Pearson's *r* correlation analysis was performed to determine if aging in normal subjects was associated with increased intereye MDB thickness asymmetry and cup-disc ratio asymmetry, and to see if both were correlated. Also, Pearson's *r* correlation analysis was used to see if spherical equivalent refractive error asymmetry in normal subjects was correlated with increasing intereye MDB thickness asymmetry. Mean MDB thickness asymmetry in OAG and normal eyes were compared using *t*-tests, globally and for all quadrants and sectors. A power calculation performed using IBM SPSS indicated 100% power to detect a statistically significant difference in mean MDB thickness asymmetry between normal and OAG subjects. In our power calculations, we determined that only 14.4 patients (or 7.2 patients per group) were needed to achieve 80% power to detect a statistically significant difference in MDB thickness asymmetry between the normal and open-angle glaucoma groups. To calculate the sample size, we used a standard deviation of 32.8 µm and used 34.3 µm as the difference between μ_1 (the average normal asymmetry difference) and μ_0 (the average glaucoma asymmetry difference). Since our study had 61 patients, the power of the final study was 100%. Absolute MDB thickness in all participants were compared using right eye MDB measurements only.

Multiple statistical methods were used to determine the best cutoff, that is, the minimum intereye MDB thickness asymmetry that could reliably distinguish OAG subjects from normal. Receiver operator characteristic (ROC) curves were calculated for average intereye MDB thickness asymmetry globally, and in all quadrants and sectors. Based on these ROC curves, the Youden's index cutoff value that maximized the sum of sensitivity and specificity for OAG diagnosis in each region was determined. The point closest to perfect classifier (PCTPC) cutoff value, which yielded sensitivity and specificity values most similar in magnitude, was also determined using the ROC curves for each ocular region. Lastly, the sensitivity and specificity of using two standard deviations above normal average intereye MDB asymmetry as the cutoff for OAG diagnosis were also determined.

IBM SPSS (IBM Corp, Armonk, NY) was used for statistical analysis. A P value of <0.05 was considered statistically significant. Measures of correction were not performed for the *t* tests because only two groups were compared (normal vs open-angle glaucoma patients).

Results

Table 1 shows the demographic and clinical characteristics of the 33 primary OAG and 28 normal subjects who met inclusion and exclusion criteria. Compared to normal subjects, OAG subjects had higher mean age (67.6 ± 10.4 vs 55.4 ± 15.8 years [P = 0.001]), greater mean cup-disc ratio asymmetry (0.11 ± 0.09 vs 0.03 ± 0.05 [P < 0.001]), lower mean deviation (−9.08 ± 5.7 dB vs −1.64 ± 1.98 dB [P < 0.001]), and higher pattern standard deviation (7.22 ± 3.7 dB vs 1.67 ± 0.47 dB [P < 0.001]). There was no significant difference in sex, race, or mean refractive error asymmetry between the groups.

Effect of Age and Refractive Error Asymmetry on MDB Neuroretinal Rim Thickness Asymmetry in Normal Subjects

Increasing age was not associated with increasing MDB neuroretinal rim thickness asymmetry or cup-disc ratio asymmetry, either globally or in quadrants or sectors; therefore, no correlation was found between them. Increasing refractive error asymmetry associated with increasing MDB thickness asymmetry was reported in the inferior quadrant (r = −0.388, P = 0.046) and superonasal sector (r = 0.409, P = 0.034) but not for the global region or other quadrants or sectors.

Digital Journal of Ophthalmology, Vol. 28

Table 1.
Demographics of the study population of patients who were imaged with spectral domain optical coherence tomography optic nerve volume scans

Study parameter	Normal	OAG	*P* value
Number of patients	28	33	
Male/female, no. (%)	10/18 (35.7/64.3)	16/17 (48.5/51.5)	0.314
Age, years, mean ± SD (range)	55.4 ± 15.8 (24-87)	67.6 ± 10.4 (46-86)	0.001
Race/ethnicity, no.			0.987
White	16	19	
Black	6	8	
Hispanic	4	4	
Asian	2	2	
Cup-disc ratio asymmetry, mean ± SD	0.03 ± 0.05	0.11 ± 0.09	<0.001
Refractive error asymmetry, mean ± SD	0.60 ± 0.8	0.57 ± 0.5	0.864
Visual field (dB), mean ± SD			
Mean deviation	−1.64 ± 1.98	−9.08 ± 5.7	<0.001
Pattern standard deviation	1.67 ± 0.47	7.22 ± 3.7	<0.001

OAG, open-angle glaucoma; *SD*, standard deviation.

Table 2.
Neuroretinal rim asymmetry in normal versus glaucomatous eyes using spectral domain optical coherence tomography volume scans

Neuroretinal rim location	Intereye MDB neuroretinal rim thickness asymmetry, µm, mean ± SD (95% CI)		*P* value
	Normal eyes	Open-angle glaucoma eyes	
Global	17.6 ± 14.2 (12.3-22.9)	51.9 ± 35.9 (39.7-64.1)	<0.001
Inferior	25.0 ± 18.0 (18.3-31.7)	81.8 ± 48.9 (65.1-98.5)	<0.001
Superior	37.1 ± 31.4 (25.5-48.7)	68.2 ± 51.1 (50.8-85.6)	0.007
Nasal	17.8 ± 14.1 (12.6-23.0)	56.2 ± 37.0 (43.6-68.8)	<0.001
Temporal	24.3 ± 23.7 (15.5-33.1)	42.2 ± 28.6 (32.4-52.0)	0.011
Inferonasal	30.7 ± 22.6 (22.3-39.1)	90.6 ± 55.2 (71.8-109.4)	<0.001
Inferotemporal	35.4 ± 25.3 (26.0-44.8)	81.0 ± 48.0 (64.6-97.4)	<0.001
Superonasal	37.5 ± 34.7 (24.6-50.4)	75.7 ± 52.2 (57.9-93.5)	0.002
Superotemporal	41.6 ± 44.2 (25.2-58.0)	76.3 ± 48.1 (59.9-92.7)	0.005

CI, confidence interval; *MDB*, minimum distance band; *SD*, standard deviation.

Differences in MDB Neuroretinal Rim Thickness Values in Subjects with Normal versus Glaucomatous Eyes

Only right eyes were used to compare normal versus glaucomatous MDB neuroretinal rim thickness. Subjects with OAG had significantly thinner mean MDB neuroretinal thickness values compared with normal eyes (209.0 µm [95% CI, 193.6–224.4 µm] vs 306.0 µm [95% CI 290.6–321.4 µm] [$P < 0.001$]).

Differences in Intereye MDB Neuroretinal Rim Thickness Asymmetry in Subjects with Normal versus Glaucomatous Eyes

Table 2 shows the neuroretinal rim asymmetry values in normal and OAG subjects. Compared with normal subjects, OAG subjects had greater intereye MDB thickness asymmetry globally and in all quadrants and sectors (Table 2). For the global region, OAG subjects had mean intereye MDB thickness asymmetry of 51.9 ± 35.9 µm (95% CI 39.7–64.1 µm) compared with 17.6 ± 14.2 µm (95% CI, 12.3–22.9 µm) for normal subjects ($P <$ 0.001). For the inferior quadrant, OAG had mean intereye MDB thickness asymmetry of 81.8 ± 48.9 µm (95%

Digital Journal of Ophthalmology, Vol. 28

Table 3.

An analysis of neuroretinal rim asymmetry using spectral domain optical coherence tomography optic nerve volume scans: three methods to determine inter-eye asymmetry cutoff values, which distinguish normal from glaucoma patients

Statistical method of cutoff determination	Scan region[a]	Cutoff, µm	Percentage exceeding cutoff		Sensitivity, % (95% CI)	Specificity, % (95% CI)
			Normal subjects[b]	OAG subjects[c]		
Youden's index–ROC curve determined cutoff[d]	G	>30.7	10.7	66.7	66.7 (48.2-82.0)	89.3 (71.8-97.7)
	S	>54.3	14.3	57.6	57.6 (39.2-74.5)	85.7 (67.3-96.0)
	T	>32.2	25.0	60.6	60.6 (42.1-77.1)	75.0 (55.1-89.3)
	N	>23.2	21.4	75.8	75.8 (57.7-88.9)	78.6 (59.0-91.7)
	I	>28.3	25.0	87.9	87.9 (71.8-96.6)	75.0 (55.1-89.3)
	ST	>56.6	21.4	69.7	69.7 (51.3-84.4)	78.6 (59.0-91.7)
	SN	>50.8	17.9	63.6	63.6 (45.1-79.6)	82.1 (63.1-93.9)
	IT	>40.3	25.0	84.8	84.8 (68.1-94.9)	75.0 (55.1-89.3)
	IN	>50.3	14.3%	72.7	72.7 (54.5-86.7)	85.7 (67.3-96.0)
Point closest to perfect classifier–ROC curve determined cutoff[e]	G	>30.7	28.6%	69.7	69.7 (51.3-84.4)	71.4 (51.3-86.8)
	S	>36.3	32.1%	66.7	66.7 (48.2-82.0)	67.9 (47.6-84.1)
	T	>29.1	35.7%	63.6	63.6 (45.1-79.6)	64.3 (44.1-81.4)
	N	>22.5	25.0%	75.8	75.8 (57.7-88.9)	75.0 (55.1-89.3)
	I	>34.5	25.0%	78.8	78.8 (61.1-91.0)	75.0 (55.1-89.3)
	ST	>48.6	28.6%	72.7	72.7 (54.5-86.7)	71.4 (51.3-86.8)
	SN	>41.7	32.1%	66.7	66.7 (48.2-82.0)	67.9 (47.6-84.1)
	IT	>51.2	25.0%	75.8	75.8 (57.7-88.9)	75.0 (55.1-89.3)
	IN	>37.9	32.1%	84.8	84.8 (68.1-94.9)	67.9 (47.6-84.1)
2 SD above normal mean MDB asymmetry thickness	G	>46.4	3.6%	48.5	48.5 (30.8-66.5	96.4 (81.7-99.9)
	S	>101.7	7.1%	27.3	27.3 (13.3-45.5)	92.9 (76.5-99.1)
	T	>70.3	3.6%	15.2	15.2 (5.1-31.9)	96.4 (81.7-99.9)
	N	>47.7	3.6%	48.5	48.5 (30.8-66.5)	96.4 (81.7-99.9)
	I	>62.2	3.6%	57.6	57.6 (39.2-74.5)	96.4 (81.7-99.9)
	ST	>127.9	3.6%	12.1	12.1 (3.4-28.2)	96.4 (81.7-99.9)
	SN	>108.2	3.6%	27.3	27.3 (13.3-45.5)	96.4 (81.7-99.9)
	IT	>88.4	3.6%	36.4	36.4 (20.4-54.9)	96.4 (81.7-99.9)
	IN	>79.2	3.6%	54.5	54.6 (36.4-71.9)	96.4 (81.7-99.9)

CI = confidence interval. *MDB*, minimum distance band, *OAG*, open-angle glaucoma; *ROC*, receiver operating characteristic; *SD*, standard deviation.

[a]*G*, global; *I*, inferior quadrant; *IN*, inferonasal sector; *IT*, inferotemporal sector; *N*, nasal quadrant; *S*, superior quadrant; *SN*, superonasal sector; *ST*, superotemporal sector; *T*, temporal quadrant.

[b]False positives misclassified as glaucoma.

[c]True positive glaucoma diagnosis.

[d]Youden's index = ROC curve–determined cutoff that maximized sum of sensitivity and specificity.

[e]Point closest to perfect classifier = ROC curve–determined cutoff that yielded greatest sensitivity and specificity that are most similar in magnitude.

CI, 65.1–98.5 µm) compared with 25.0 ± 18.0 µm (95% CI, 18.3–31.7 µm) for normal subjects ($P < 0.001$); and for the inferonasal sector, OAG had mean intereye MDB thickness asymmetry of 90.6 ± 55.2 µm (95% CI, 71.8–109.4 µm) compared with 30.7 ± 22.6 µm (95% CI, 22.3–39.1 µm) for normal subjects ($P < 0.001$).

Determination of Neuroretinal Rim Asymmetry Cutoff Values to Distinguish Subjects with Normal versus Glaucomatous Eyes—Comparison of Three Statistical Methods

Table 3 shows the cutoff values that best distinguish normal from glaucomatous subjects, using three statistical methods. With Youden's index, global MDB thickness

Digital Journal of Ophthalmology, Vol. 28

asymmetry >30.7 μm yielded the greatest sum of sensitivity (66.7%; 95% CI, 48.2%-82.0% [$P < 0.001$]) and specificity (89.3%; 95% CI, 71.8–97.7 μm [$P < 0.001$]) for detecting OAG based on global MDB measurements. Among all regions, the inferior quadrant yielded the cutoff value with the greatest sum (87.9%, 95% CI 71.8%–96.6% [$P < 0.001$]) and specificity (75.0%; 95% CI, 55.1%–89.3% [$P < 0.001$]).

Using the PCTPC, global MDB thickness asymmetry >30.7 μm yielded sensitivity (69.7%; 95% CI, 51.3%–84.4% [$P < 0.001$]) and specificity (71.4%; 95% CI 51.3%–86.8% [$P < 0.001$]) that were most similar in magnitude for detecting OAG based on global MDB measurements (Table 3). For the inferior quadrant, MDB thickness asymmetry >34.5 μm yielded a sensitivity of 78.8% (95% CI, 61.1%–91.0% [$P < 0.001$]) and specificity of 75.0% (95% CI, 55.1%–89.3% [$P < 0.001$]).

Using two standard deviations above normal mean global MDB thickness asymmetry, global MDB thickness asymmetry >46.4 μm yielded 48.5% sensitivity (95% CI, 30.8%–66.5% [$P < 0.001$]) and 96.4% specificity (95% CI, 81.7%–99.9% [$P < 0.001$]) for detecting OAG based on global MDB measurements (Table 3). In the inferior quadrant, MDB thickness asymmetry >62.2 μm yielded 57.6% sensitivity (95% CI, 39.2%–74.5% [$P < 0.001$]) and 96.4% specificity (95% CI, 81.7%–99.9% [$P < 0.001$]) for detecting OAG.

Of the three methods, Youden's index provided the greatest combined sensitivity and specificity (Table 3): cutoff values were able to detect more glaucoma cases (57.6%–87.9%) with fewer false positives (10.7%–25.0%) than the other methods. Although the PCTPC cutoff values detected a similar percentage of glaucoma patients (63.6%–84.8%), there were more false positives (25.0%–35.7%). The highest global cutoff value (46.4 μm) was determined as two standard deviations above the normal mean MDB asymmetry value. This highest cutoff value had low sensitivity (48.5%; 95% CI, 30.8%–66.5%) but was associated with the fewest false positives (3.6%) of any cutoff value (Table 3).

Discussion

To our knowledge, this is the first study to demonstrate that SD-OCT volume scans with neuroretinal rim tissue asymmetry can aid in distinguishing normal eyes from glaucomatous eyes in a multi-ethnic population. Prior intereye asymmetry papers had focused on asymmetry of the RNFL, vessel density, or macular thickness.[2,4,5,7,20,21] This study suggests that 3D OCT global neuroretinal rim asymmetry >30.7 μm may be a strong indicator of glaucoma (ie, sensitivity of 66.7% [95% CI, 48.2%–82.0%] and specificity of 89.3% [95% CI, 71.8%–97.7%]). Similarly, the inferior quadrant intereye asymmetry >28.3 μm supports a diagnosis of glaucoma with 87.9% sensitivity (95% CI, 71.8%–96.6%) and 75.0% specificity (95% CI, 55.1%–89.3%). Unlike traditional subjective analysis of disc asymmetry, 3D SD-OCT objectively quantifies asymmetry, a hallmark of early glaucomatous change.[13]

Although two-dimensional (2D) RNFL thickness is the most commonly used SD-OCT parameter in the evaluation of glaucoma patients, it has significant limitations. First, glaucoma causes the RNFL to become less reflective, making accurate identification and segmentation of the RNFL borders more difficult.[15,22] As a result, RNFL scans carry a high rate of artifacts, with 7.1%–61.7% of scans affected [15,16,23–25] compared with only 15.8% with the MDB parameter.[16] Second, RNFL scans are prone to false positives results from conditions such as myopia, which cause RNFL thinning unrelated to glaucoma.[26–28] Third, the age-matched normative database to which RNFL thickness measurements are compared does not account for normal ethnic variations.[29,30]

In contrast, 3D neuroretinal rim measurements (ie, high-density MDB thickness and low-density BMO-MRW) may better overcome some of the aforementioned limitations of the most commonly used RNFL thickness measurement. Specifically, compared to the traditional RNFL thickness measurement, 3D neuroretinal rim measurements: (1) have equal or better diagnostic ability for glaucoma,[11,13] (2) have fewer clinically significant artifacts (ie, 15.8% vs 61.7%),[16] and (3) are less affected by myopia.[31,32] Lastly, a recent 5-year longitudinal study demonstrated that high-density MDB neuroretinal rim measurements can detect glaucoma progression 1 to 2 years earlier than current commercially available structural tests (ie, disc photographs and RNFL thickness).[14]

In our study, the OAG subjects had significantly greater global intereye neuroretinal MDB thickness asymmetry than normal subjects, and the MDB neuroretinal rim was thinner in glaucoma patients compared to normal patients (ie, 209 μm ± 45 μm vs 306 μm ± 42 μm [$P < 0.001$]; Tables 1 and 2). Glaucoma patients also had greater interocular neuroretinal rim asymmetry than normal patients in all quadrants and all sectors (ie, difference >30.7 μm globally [66.7% sensitivity, 89.3% specificity], >28.3 μm in the inferior quadrant [87.9% sensitivity, 75.0% specificity]; Tables 2–3). Of the three statistical methods to determine best cutoff values that differentiate normal from glaucomatous eyes, the Youden index provided the greatest combined sensitivity and

Digital Journal of Ophthalmology, Vol. 28

specificity (Table 3); cutoff values detected more glaucoma cases (57.6%–87.9%) with fewer false positives (10.7%–25.0%) than the other method.

Besides global intereye asymmetry, this study also showed that the inferior quadrant, which includes the inferior nasal sector and inferior temporal sector, has the greatest intereye MDB asymmetry in glaucoma, when compared to other quadrants and sectors (Table 3). This is most likely due to the tendency of early glaucoma to preferentially cause superior and inferior thinning of the neuroretinal rim.[33,34] When determining asymmetry cut-off values to distinguish between normal and glaucoma patients for specific quadrants and sectors (Table 3), all three methods consistently showed the best combinations of sensitivities and specificities for the inferior, inferior temporal, and inferior nasal regions (Youden's index: inferior, inferior temporal, inferior nasal; PCTPC-ROC curve determined cut-off: inferior, inferior nasal; 2 standard deviations above the normal mean MDB asymmetry thickness: inferior, inferior nasal). Although good diagnostic ability for the inferior temporal location for rim asymmetry fits well with classic teaching that the inferior temporal nerve tissue is preferentially damaged in early glaucoma, it was more surprising to see that the inferior nasal rim location also had good diagnostic ability (inferonasal 90.6 ± 55.2 μm [95% CI, 71.8–109.4 μm] vs inferotemporal 81.0 ± 48.0 μm [95% CI, 64.6–97.4 μm]; Table2). In theory, the best diagnostic parameter is one that has a large dynamic range but that does not have a wide range of normal values that overlaps with glaucoma values. For the neuroretinal rim and for the first criteria of a larger dynamic range, we hypothesize that the inferior nasal rim is normally thicker than the inferior temporal rim, per the ISNT rule. The ISNT rule describes the normal neuroretinal rim, which can be thickest inferiorly (I), then thinner superior (S), then thinner nasally (N), and thinnest temporally (T). Deviations from the ISNT rule may suggest glaucomatous changes. In contrast, the inferior temporal and superior temporal RNFL is normally thicker than the inferior nasal and superior nasal RNFL, as demonstrated by most OCT RNFL thickness maps. For the neuroretinal rim, and for the second criteria of less normal variability, we hypothesize that the inferior nasal sector may have less normal variability than the inferior temporal or superior temporal sectors, which may have more normal variability in patients with normal temporal sloping of the neuroretinal rim. Future studies could prove or disprove these theories.

Overall, interocular MDB asymmetry had similar sensitivity and specificity (Table 3) to RNFL asymmetry as a diagnostic tool for OAG.[2,4] Sullivan-Mee et al[2] found that global RNFL thickness asymmetry had the greatest combined sensitivity (82.4%) and specificity (80.0%) compared to other regions, both with 95% CI of 84.9%–96.5%. Field et al[4] also reported that global RNFL thickness asymmetry had greatest combined sensitivity (74.2%; 95% CI, 65.9%–82.5%) and specificity (90.0%; 95% CI, 84.3%–95.7%), with the inferior quadrant showing the second greatest difference between OAG and normal eyes. The Sullivan-Mee and Field RNFL studies had similar combined sensitivities and specificities to those found in our study for global MDB asymmetry (Table 3; Youden index's, sensitivity 66.7% with 95% CI of 48.2%–82.0% and specificity 89.3% with 95% CI of 71.8%–97.7%). Of the three methods (Table 3), when we used the most stringent and highest cut-off value for global MDB thickness asymmetry (ie, > 46.4 μm, or 2 standard deviations above the normal mean MDB thickness asymmetry), the best specificity was achieved (96.4%; 95% CI 81.7%–99.99%), but this was associated with a low sensitivity of 48.5% (95% CI 30.8%–66.5%). Field et al[4] similarly found that a cut-off of 2 standard deviations above the normal mean global RNFL thickness asymmetry had 95.0% specificity and 51.5% sensitivity. Sullivan-Mee et al[2] reported 66.0% sensitivity when specificity was 95% in detecting OAG by global RNFL thickness asymmetry. Thus, both SD-OCT-based MDB thickness asymmetry and RNFL thickness asymmetry parameters can achieve high specificity at the expense of low sensitivity when higher cut-offs are used. Because of its improved detection of OAG in myopic patients and independence from glaucoma-related reflectivity changes, neuroretinal rim MDB asymmetry may be a more robust parameter than RNFL asymmetry.[11,13,15]

Our study has limitations. We did not include subjects with pre-perimetric glaucoma. Additionally, the relatively small sample size precluded a more detailed analysis of the normal ethnic variations in neuroretinal MDB thickness. Further studies are needed to establish a larger normative database in order to better assess for possible normal racial variations.[35] A larger study would also be needed to determine whether results would vary based on glaucoma staging (ie, early, moderate, or late stage glaucoma). Our study also cannot fully evaluate the effects of high myopia on neuroretinal MDB measurements, because we excluded patients with myopia of > −5.0 D from the study. Lastly, normal subjects were not age-matched with OAG subjects, who were older. However, most glaucoma imaging studies, including this one, do not have age-matched controls, because expected age-related decline of OCT imaging metrics is usually

Digital Journal of Ophthalmology, Vol. 28

less than expected inter-test measurement variability. Since OCT glaucoma progression is defined as a change greater than both normal aging change and expected inter-test variability, age-related changes usually are not clinically significant and usually do not need to be factored in.

In summary, our findings indicate that the MDB neuroretinal rim is thinner in glaucoma patients and that inter-eye neuroretinal MDB asymmetry measurements using high-density SDOCT volume scans is a highly sensitive, specific method for detecting OAG. It could potentially serve as a reliable, objective, and quantitative tool for open-angle glaucoma diagnosis.

References

1. Chen TC, Zeng A, Sun W, Mujat M, de Boer JF. Spectral domain optical coherence tomography and glaucoma. Int Ophthalmol Clin 2008;48:29-45.
2. Sullivan-Mee M, Ruegg CC, Pensyl D, Halverson K, Qualls C. Diagnostic precision of retinal nerve fiber layer and macular thickness asymmetry parameters for identifying early primary open-angle glaucoma. Am J Ophthalmol 2013;156:567-77.e561.
3. Chen MJ, Yang HY, Chang YF, Hsu CC, Ko YC, Liu CJ. Diagnostic ability of macular ganglion cell asymmetry in preperimetric glaucoma. BMC Ophthalmol 2019;19:12.
4. Field MG, Alasil T, Baniasadi N, et al. Facilitating glaucoma diagnosis with intereye retinal nerve fiber layer asymmetry using spectral-domain optical coherence tomography. J Glaucoma 2016;25:167-76.
5. Gupta D, Asrani S. Macular thickness analysis for glaucoma diagnosis and management. Taiwan J Ophthalmol 2016;6:3-7.
6. Hou H, Moghimi S, Zangwill LM, et al. Inter-eye asymmetry of optical coherence tomography angiography vessel density in bilateral glaucoma, glaucoma suspect, and healthy eyes. Am J Ophthalmol 2018;190:69-77.
7. Mwanza JC, Durbin MK, Budenz DL, Cirrus OCT Normative Database Study Group. Interocular symmetry in peripapillary retinal nerve fiber layer thickness measured with the Cirrus HD-OCT in healthy eyes. Am J Ophthalmol 2011;151:514-21.e511.
8. Yamada H, Hangai M, Nakano N, et al. Asymmetry analysis of macular inner retinal layers for glaucoma diagnosis. Am J Ophthalmol 2014;158:1318-29.e1313.
9. Zangalli CES, Reis ASC, Vianna JR, Vasconcellos JPC, Costa VP. Interocular asymmetry of minimum rim width and retinal nerve fiber layer thickness in healthy Brazilian individuals. J Glaucoma 2018;27:1136-41.
10. Shieh E, Lee R, Que C, et al. Diagnostic performance of a novel three-dimensional neuroretinal rim parameter for glaucoma using high-density volume scans. Am J Ophthalmol 2016;169:168-78.
11. Tsikata E, Lee R, Shieh E, et al. Comprehensive three-dimensional analysis of the neuroretinal rim in glaucoma using high-density spectral-domain optical coherence tomography volume scans. Invest Ophthalmol Vis Sci 2016;57:5498-508.
12. Celebi ARC, Park EA, Verticchio Vercellin AC, et al. Structure-function mapping using a three-dimensional neuroretinal rim parameter derived from spectral domain optical coherence tomography volume scans. Transl Vis Sci Technol 2021;10:28.
13. Chauhan BC, O'Leary N, AlMobarak FA, et al. Enhanced detection of open-angle glaucoma with an anatomically accurate optical coherence tomography-derived neuroretinal rim parameter. Ophthalmology 2013;120:535-43.
14. Ratanawongphaibul K, Tsikata E, Zemplenyi M, et al. Earlier detection of glaucoma progression using high-density 3-dimensional spectral-domain OCT optic nerve volume scans. Ophthalmol Glaucoma 2021;4:604-16.
15. Liu Y, Simavli H, Que CJ, et al. Patient characteristics associated with artifacts in spectralis optical coherence tomography imaging of the retinal nerve fiber layer in glaucoma. Am J Ophthalmol 2015;159:565-76.e562.
16. Park EA, Tsikata E, Lee JJ, et al. Artifact rates for 2D retinal nerve fiber layer thickness versus 3D neuroretinal rim thickness using spectral-domain optical coherence tomography. Transl Vis Sci Technol 2020;9:10.
17. Kim J, Men CJ, Ratanawongphaibul K, et al. Reproducibility of neuroretinal rim measurements obtained from high-density spectral domain optical coherence tomography volume scans. Clin Ophthalmol 2022;16:2595-608.
18. Mwanza JC, Budenz DL. New developments in optical coherence tomography imaging for glaucoma. Curr Opin Ophthalmol 2018;29:121-9.
19. Wu H, de Boer JF, Chen TC. Diagnostic capability of spectral-domain optical coherence tomography for glaucoma. Am J Ophthalmol 2012;153:815-26.e812.
20. Chauhan BC, Hangai M, Iwase A, et al. Bruch's membrane opening-based neuroretinal rim width and retinal nerve fibre layer thickness in a normal Japanese population: a multi-centre study [abstract]. Invest Ophthalmol Vis Sci 2015;56:1014.
21. Dave P, Jethani J, Shah J. Asymmetry of retinal nerve fiber layer and posterior pole asymmetry analysis parameters of spectral domain optical coherence tomography in children. Semin Ophthalmol 2017;32:443-8.
22. Chen TC. Spectral domain optical coherence tomography in glaucoma: qualitative and quantitative analysis of the optic nerve head and retinal nerve fiber layer (an AOS thesis). Trans Am Ophthalmol Soc 2009;107:254-81.
23. Asrani S, Essaid L, Alder BD, Santiago-Turla C. Artifacts in spectral-domain optical coherence tomography measurements in glaucoma. JAMA Ophthalmol 2014;132:396-402.
24. Choi S, Jassim F, Tsikata E, et al. Artifact rates for 2d retinal nerve fiber layer thickness versus 3D retinal nerve fiber layer volume. Transl Vis Sci Technol 2020;9:12.
25. Nakano N, Hangai M, Noma H, et al. Macular imaging in highly myopic eyes with and without glaucoma. Am J Ophthalmol 2013;156:511-23.e516.
26. Kang SH, Hong SW, Im SK, Lee SH, Ahn MD. Effect of myopia on the thickness of the retinal nerve fiber layer measured by Cirrus HD optical coherence tomography. Invest Ophthalmol Vis Sci 2010;51:4075-83.
27. Kimura Y, Hangai M, Morooka S, et al. Retinal nerve fiber layer defects in highly myopic eyes with early glaucoma. Invest Ophthalmol Vis Sci 2012;53:6472-8.
28. Leung CK, Mohamed S, Leung KS, et al. Retinal nerve fiber layer measurements in myopia: an optical coherence tomography study. Invest Ophthalmol Vis Sci 2006;47:5171-6.
29. Tsai CS, Zangwill L, Gonzalez C, et al. Ethnic differences in optic nerve head topography. J Glaucoma 1995;4:248-57.
30. Zangwill LM, Weinreb RN, Berry CC, et al. Confocal Scanning

Laser Ophthalmoscopy Ancillary Study to the Ocular Hypertension Treatment Study. Racial differences in optic disc topography: baseline results from the confocal scanning laser ophthalmoscopy ancillary study to the ocular hypertension treatment study. Arch Ophthalmol 2004;122:22-8.

31. Sanfilippo PG, Huynh E, Yazar S, Hewitt AW, Mackey DA. Spectral-domain optical coherence tomography-derived characteristics of Bruch membrane opening in a young adult Australian population. Am J Ophthalmol 2016;165:154-63.
32. Nicolela MT, Malik R, Belliveau A, et al. Improved diagnostic performance of an optical coherence tomography-derived neuroretinal rim parameter in myopic eyes. Invest Ophthalmol Vis Sci 2014;55:4026.
33. Kanamori A, Nakamura M, Escano MF, Seya R, Maeda H, Negi A. Evaluation of the glaucomatous damage on retinal nerve fiber layer thickness measured by optical coherence tomography. Am J Ophthalmol 2003;135:513-20.
34. Nouri-Mahdavi K, Hoffman D, Tannenbaum DP, Law SK, Caprioli J. Identifying early glaucoma with optical coherence tomography. Am J Ophthalmol 2004;137:228-35.
35. Antar H, Tsikata E, Ratanawongphaibul K, et al. Analysis of neuroretinal rim by age, race, and sex using high-density 3-dimensional spectral-domain optical coherence tomography. J Glaucoma 2019;28:979-88.

Digital Journal of Ophthalmology, Vol. 28